

Response to Anonymous Referee #3

Authors' responses to reviewer comments after major revision appear in purple text.

We would like to express our sincere gratitude to the referee for their valuable time and effort in reviewing our paper, as well as for their insightful suggestions.

Authors' responses to reviewer comments appear in blue text. Line numbers referenced in the authors' responses refer to the revised document. Figures with Arabic numerals (e.g., Figure 10) correspond to the revised manuscript; figures with Roman numerals (e.g., Figure iv) only appear in response to the reviewer's comments.

The present studies are intended at investigating the wake characteristics of a balloon wind turbine using an actuator disk theory solved through an LES solver. Although the topic itself is of interest, I do feel the authors need to improve the paper for publication. The following aspects are some comments from my side:

1. The authors provide too detailed formulations on the LES and actuator disk theories while they do not attempt to improve them. These can be omitted.

Thank you for your feedback. We have carefully considered your comment and made revisions to reduce the extent of this section while still ensuring clarity and comprehension. The governing equations of LES and sub-grid stress model for turbulence modeling were removed from section 2. General descriptions of Momentum and Balde element theories were eliminated from sections 3.1 and 3.2. Moreover, primary equations in these theories, i.e., equations 1, 2, 13, 14, and 15, and their descriptions were eliminated from the sections. Nevertheless, the secondary equations resulting from the substitution of various variables in these equations were retained to convey the fundamental principles of the BEM theory.

2. Numerical description is too weak. The authors shall provide more information about the approaches used to solve the sets of flow equations, e.g., time integration? discretization? convergence acceleration?

We added more information about the simulation set up in Line (210) of the manuscript as follows:

Line (210): The PISO scheme was utilized for pressure-velocity coupling. This scheme is well-suited for unsteady and highly transient flows, which are characteristic of wind turbine wake simulations. For spatial discretization of pressure and momentum, the second-order form and the time integration, the second-order implicit, were employed to improve the stability and convergence of the simulations. Simulations ran for a maximum of 20 iterations per time step, using a convergence criterion of 1×10^{-4} for the residuals in all cases.

To further elaborate on the previous details of the simulation setup, we decided to provide more information about the convergence acceleration method used in our research. Following is the updated description of numerical settings in the manuscript:

Line (210): The PISO scheme was utilized for pressure-velocity coupling. This scheme is well-suited for unsteady and highly transient flows, which are characteristic of wind turbine wake simulations. For spatial discretization of pressure and momentum, the second-order form and the time integration, the second-order implicit, were employed to improve the stability and convergence of the simulations. Simulations ran for a maximum of 20 iterations per time step, using a convergence criterion of 1×10^{-4} for the residuals in all cases. Obtaining convergence in unsteady wind turbine wake simulations is time-consuming. To expedite the convergence process while maintaining stability, under-relaxation techniques, including the application of factors of 0.3 to the pressure equation and 0.7 to the momentum equation, were employed.

3. Temporal discretization studies are not performed. How can we sure the solutions are accurate with respect to time size?

Due to the inherent complexity and computational demands of LES, conducting a comprehensive investigation into the accuracy with respect to time size would have imposed significant limitations on our computational resources. However, we would like to emphasize that we took steps to ensure the accuracy and convergence of our simulations in terms of the time step size. Sensitivity studies were conducted to assess the impact of the time step size on the convergence of the simulations. After careful consideration, we selected a maximum time step required for the simulations to converge, which was approximately close to the time required for a rotor rotation of 2.5 degrees ($\Delta t = 0.0016$ s).

The criterion used for the computation of the time step was added to Line (215) of the manuscript as follows:

Line (215): The size of the time step was selected after sensitivity studies to assess the impact of the time step size on the convergence. To avoid excessive computational costs, the maximum time step required for the simulations to converge was selected, which was approximately close to the time required for a rotor rotation of 2.5 degrees ($\Delta t = 0.0016$ s). LES calculations were run sufficiently to reach stable statistics of the flow.

In response to your query regarding the criterion employed for determining the time step, we wish to provide a comprehensive view of our approach. Initially, we considered multiple methods for selecting the time step size, including an evaluation of the independence of results from the time step and an assessment against the minimum flow time scale in critical regions. However, after careful deliberation and consideration of our computational resources, we opted to primarily rely on the convergence criterion. This decision was driven by the merits of the convergence criterion, which had a robust track record and was meticulously established through sensitivity studies to ensure both the stability and accuracy of our simulations. Nonetheless, we present the results of our additional methods here to underscore the robustness and reliability of our approach.

1. Independence of the results from the selected time step:

To address this, we duplicated a similar simulation setup as detailed in Section 4 of our paper, with U_{ref} set to 7 and θ_{tilt} at 0° . We conducted simulations employing smaller time steps (specifically, 0.0004 s and 0.008 s) compared to the time step used in the original simulations. It is important to note that when using larger time steps, we encountered numerical instability that failed to meet the convergence criterion. Figure i illustrates the vertical profiles of the time-averaged normalized x-velocity at various positions downstream of the wind turbine, spanning the range of $-4 < y/d < 4$ at $z = 0$.

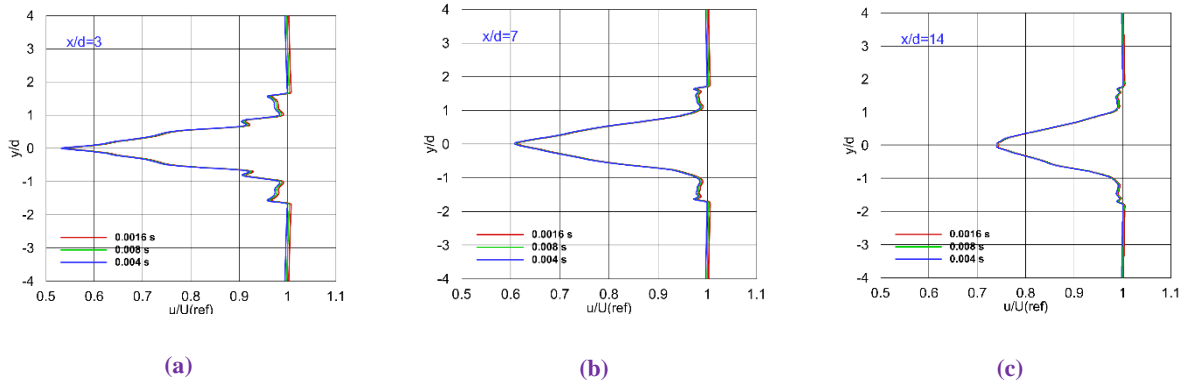


Figure i. Comparison of vertical profiles of the time-averaged normalized x-velocity for different time steps for $U_{\text{ref}}=7$ m s^{-1} and $-4 < y/d < 4$, and $z=0$ with $\theta_{\text{tilt}}=0^\circ$ at (a) $x/d=3$ (b) $x/d=7$ (c) $x/d=14$

According to figure i, the difference in the time-averaged normalized x-velocity at $x/d = 3$ for simulations using $\Delta t = 0.0016$ s and $\Delta t = 0.004$ s is found to be below 1 percent. Moreover, this difference further diminishes in downstream locations. The negligible variation observed between the original time step and the smaller time steps demonstrates that the chosen Δt is sufficiently small to accurately capture the intricate details of the flow. This includes the representation of small-scale turbulent features and the unsteady behaviour of the wake, which are directly linked to the precise prediction of velocity deficits in the wake region.

2. Time scale method:

The selected time step was then assessed to ensure it remained lower than or close to the smallest time scale governing the flow dynamics within our critical areas of interest —specifically, in the wake zone and the vicinity of the balloon. In this refined approach, we considered cells within these regions with the largest edge length (Δx) and local average velocity (V). We aimed to ensure that our time step (Δt) was sufficiently small to provide the necessary temporal resolution to accurately capture the flow's behaviour as it traversed these cells ($\Delta t \leq \Delta x / V$). In this regard, LES calculations were run sufficiently to reach stable statistics of the flow. The time scale was then computed using Eq. (1). Time scale contours in the iso-clipped symmetry plan of the balloon ($z=0$ and $-9 < y < 9$) for $U_{\text{ref}} = 7, 10 \text{ m s}^{-1}$ and $\theta_{\text{tilt}} = 0^\circ$ are shown in figure ii.

$$\text{Time scale} = \frac{\text{cell volume}^{\frac{1}{3}}}{|V|} \quad (1)$$

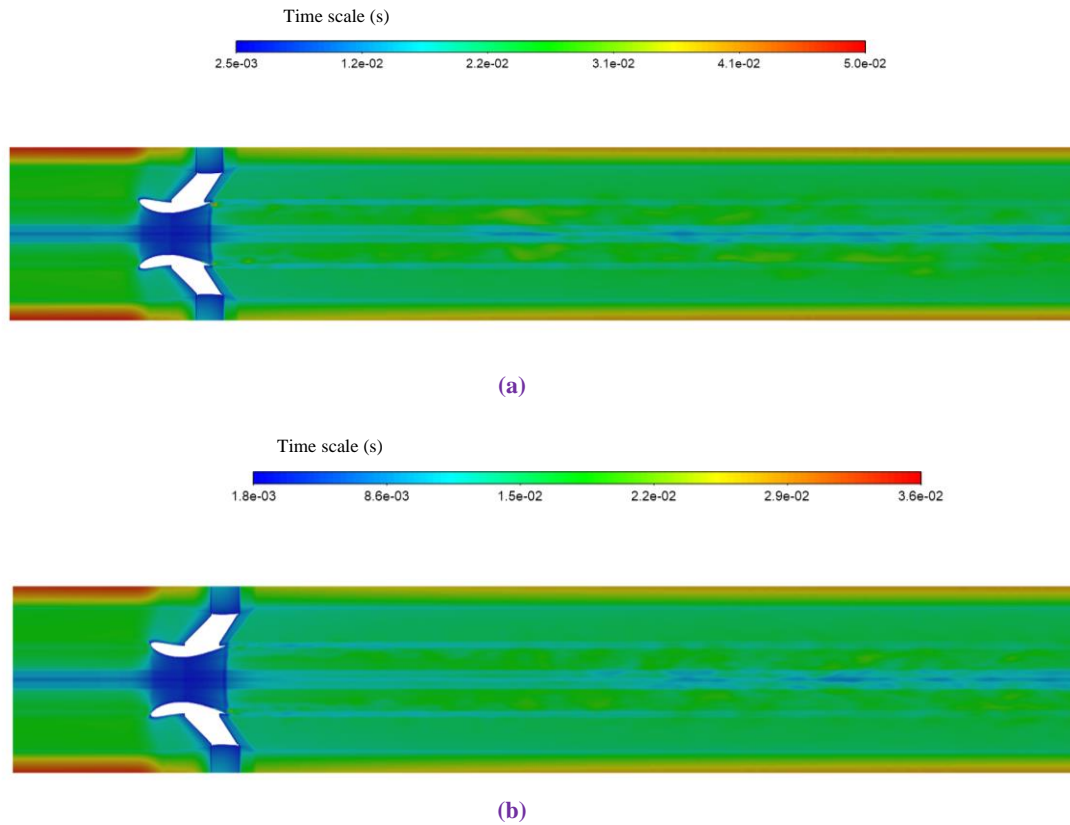


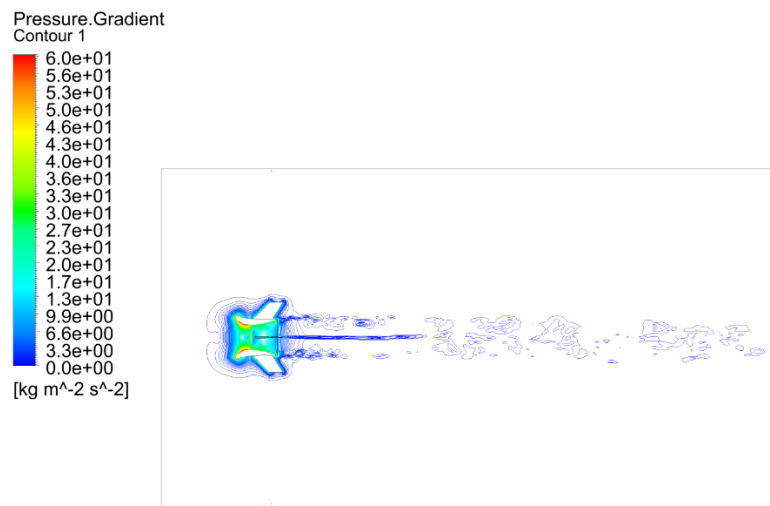
Figure ii. Time scale contours in the iso-clipped symmetry plan of the balloon ($z=0$ and $-9 < y < 9$) for $\theta_{tilt} = 0^\circ$ (a) $U_{ref} = 7 \text{ m s}^{-1}$ and (b) $U_{ref} = 10 \text{ m s}^{-1}$

As depicted in figure ii, the minimum time scale within the wake region and surrounding the balloon remains within the range of 0.0025 seconds for $U_{ref} = 7 \text{ m s}^{-1}$ and 0.0018 seconds for $U_{ref} = 10 \text{ m s}^{-1}$, which falls comfortably below the time step determined through sensitivity studies for convergence (0.0016 seconds). Further examination of the time scale and independence of the results from the selected time step under varying conditions, specifically for $\theta_{tilt} = 5^\circ$ and 10° at both inlet reference velocities, serves to confirm that the chosen time step aligns with both aforementioned criteria.

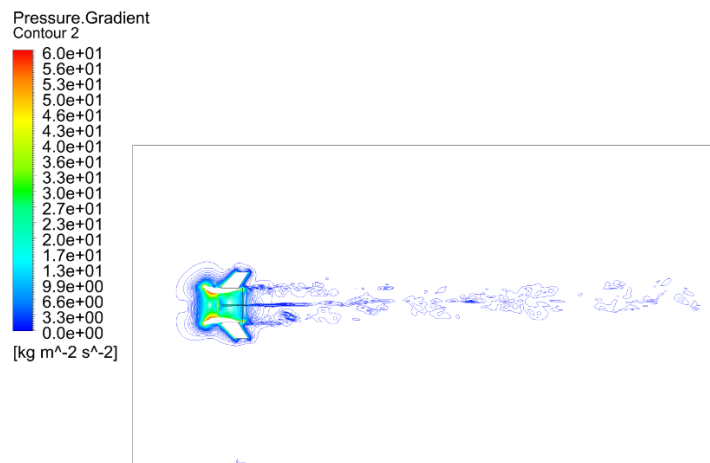
4. Upstream domain looks a bit too small.

To complete the determination of the domain dimensions, it was solved separately by different domain sizes and observing the variable flow gradients at the boundaries. The computational domain was chosen as the minimum size that exhibited zero gradients at the boundaries. Figure iii illustrates the pressure gradients for $U_{ref} = 7 \text{ m s}^{-1}$ and $\theta_{tilt} = 0^\circ, 5^\circ$ and 10° on a symmetry plane of the balloon in the finalized domain. The pressure contours provide an evident indication that

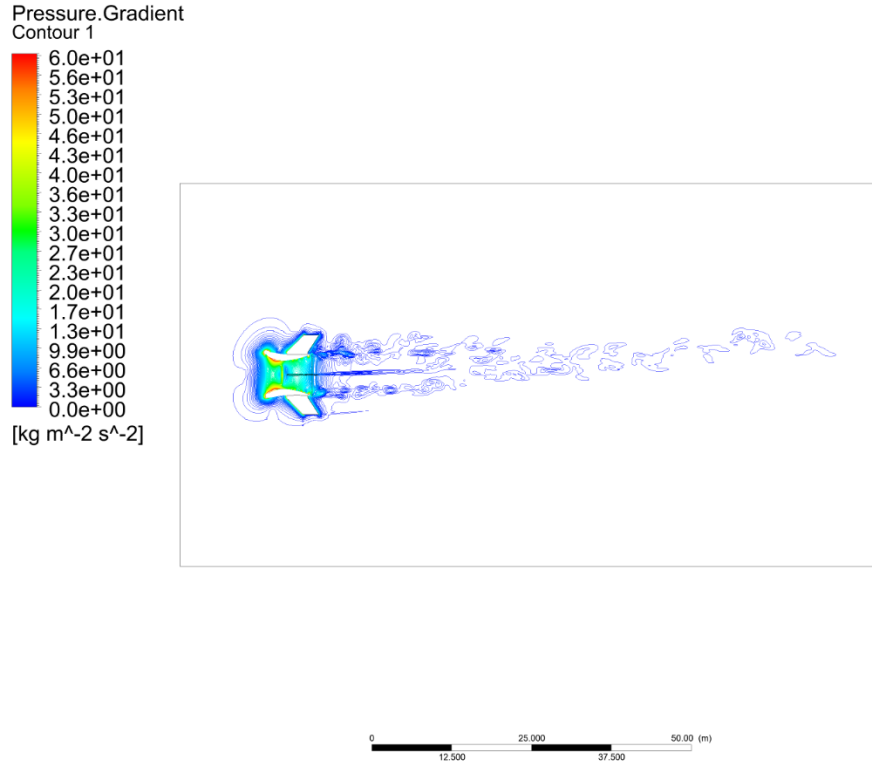
there is no pressure gradient present at the boundary of the domain with the determined dimensions.



(a)



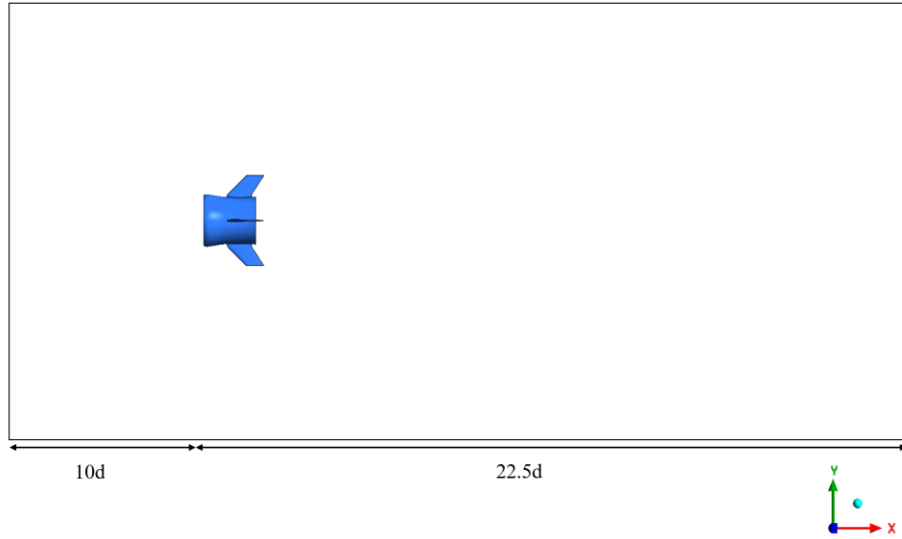
(b)



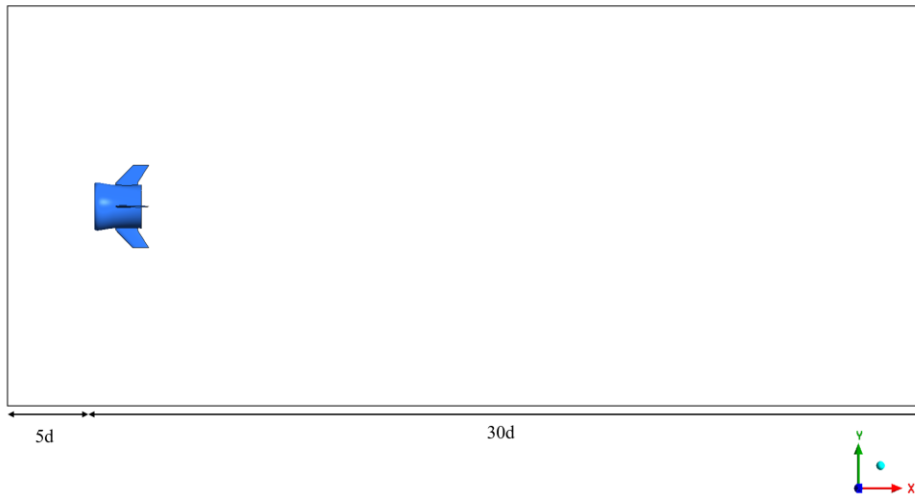
(c)

Figure iii. Pressure gradient contour for $U_{ref} = 7 \text{ m s}^{-1}$ and (a) $\theta_{tilt} = 0^\circ$, (b) $\theta_{tilt} = 5^\circ$ (c) $\theta_{tilt} = 10^\circ$ on the symmetry plane of the balloon ($z=0$).

In response to the referee's query regarding the sensitivity of the computational domain size, we would like to provide additional information to further support the appropriateness of the domain size chosen in our study. In our initial response, we explained that the domain dimensions were carefully determined by evaluating flow gradients at the boundaries, to select a size that ensured zero gradients. While this method was valid, we employed sensitivity analysis of wake characteristics in relation to domain size here to further support the reliability of our approach. In light of this, we have conducted a follow-up study wherein we created two different computational domains: one with an extended upstream length (from 5d to 10d) and another with an extended downstream length (from 22.5d to 30d) as shown in figure iv relative to the turbine position, beyond the original domain utilized in the research. We increased the number of nodes in the upstream distance by a factor of 2 for the extended upstream domain and by 1.3 times (equal to the length increment ratio) for the extended downstream domain to ensure consistent spatial resolution in all cases, while only considering changes in the computational domain size on the results.



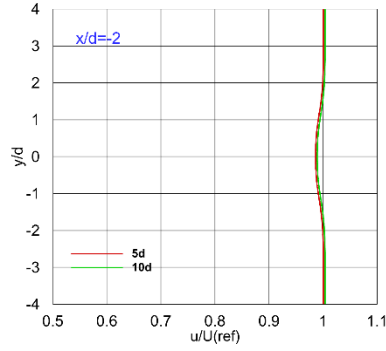
(a)



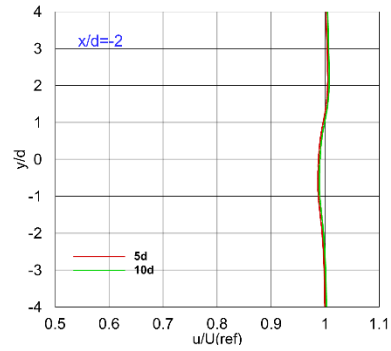
(b)

Figure iv. Computational domain size for (a) extended upstream length and (b) extended downstream length.

With these new computational domains, we applied the same simulation settings and boundary conditions as described in Section 4 of the paper to conduct simulations for the cases where $U_{\text{ref}} = 7 \text{ m s}^{-1}$ and $\theta_{\text{tilt}} = 0^\circ$ and 10° . Figure v showcases the simulation results employing an extended upstream length, illustrating vertical profiles of the time-averaged normalized x-velocity at $x/d = -2$, within the range of $-4 < y/d < 4$ at $z = 0$. Additionally, figure vi presents the outcomes of the simulation utilizing an extended downstream length, displaying vertical profiles of the time-averaged normalized x-velocity at $x/d = 5$ and 14 , within the range of $-4 < y/d < 4$ at $z = 0$.

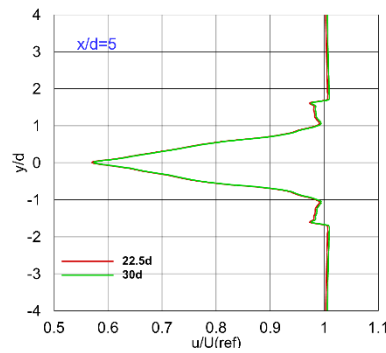


(a)

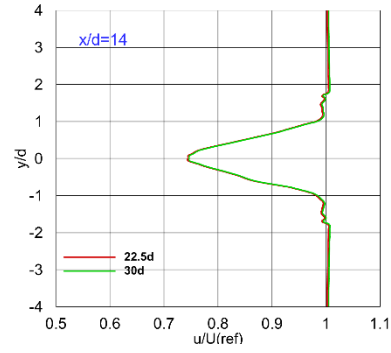


(b)

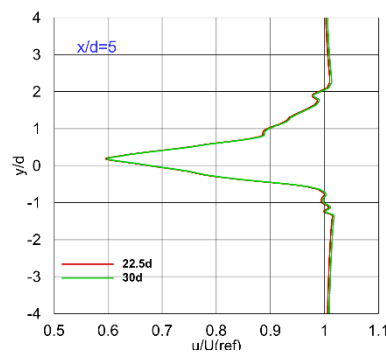
Figure v. Comparison of vertical profiles of the time-averaged normalized x-velocity for different upstream lengths for $U_{ref}=7 \text{ m s}^{-1}$ and $-4 < y/d < 4$, and $z=0$ with $\theta_{tilt} =$ (a) 0° (b) 10° at $x/d = -2$.



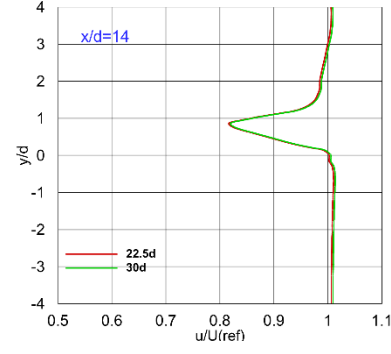
(a)



(b)



(c)



(d)

Figure vi. Comparison of vertical profiles of the time-averaged normalized x-velocity for different downstream lengths for $U_{ref}=7 \text{ m s}^{-1}$ and $-4 < y/d < 4$, and $z=0$ with $\theta_{tilt} = 0^\circ$ at (a) $x/d = 5$ (b) $x/d = 14$ and $\theta_{tilt} = 10^\circ$ at (c) $x/d = 5$ (d) $x/d = 14$.

According to figure v, extending upstream lengths has been observed to have a relatively minor impact on the velocity profiles at various locations relative to the wind turbine position. This observation can be ascribed to the specific conditions governing our investigation. Notably, we considered our wind turbine situated at a high altitude where the atmosphere tends to be more stable because it is less influenced by surface heating and friction, which can lead to reduced turbulence and vertical mixing. The absence of significant boundary layer effects due to the high-altitude location of our wind turbine led to a longer upstream length less critical for capturing boundary layer-related phenomena. These specific environmental conditions enabled us to design our computational domain with a smaller upstream length than typically required for studying ground-based wind turbine wake behaviour, prioritizing computational efficiency while maintaining result accuracy.

Furthermore, as shown in figure vi, prolonging the downstream distances has shown only a marginal influence on the velocity profiles at different positions relative to the wind turbine's location. Our choice of downstream length was carefully considered in light of several critical factors. The selected downstream domain size was designed to encompass the essential characteristics of the wake, including wake recovery, turbulence decay, and gradual mixing with ambient air. This careful consideration of downstream length was paramount to accurately capturing the wake's behaviour and its impact on downstream flow. In summary, under these controlled conditions and with careful attention to factors critical to wake simulation, the impact of extending the domain size upstream and downstream remained minimal, providing robust support for the appropriateness of our chosen computational domain size.

5. Validation studies use conventional wind turbines, while the case being studied is much more complex.

Due to the novelty of balloon wind turbines, there is a lack of experimental data in the literature to validate the numerical results pertaining to their aerodynamics and wake flow. Nevertheless, it is possible to assess the methodology employed in this study to characterize the wake flow of these turbines. To this end, we employed the same methodology to investigate the wake behaviour of a smaller turbine that had been previously studied experimentally.

There are two key differences between the balloon wind turbine and the smaller turbine: the diameter of their rotors and the presence of the balloon in the main model. Based on the results obtained from the balloon wind turbine, it is evident that the effective length of the rotor wake is considerably longer than that of the balloon, and they do not interact under various inflow conditions considered in this study. Hence, the wake flow behaviour of the rotor is almost independent of the balloon.

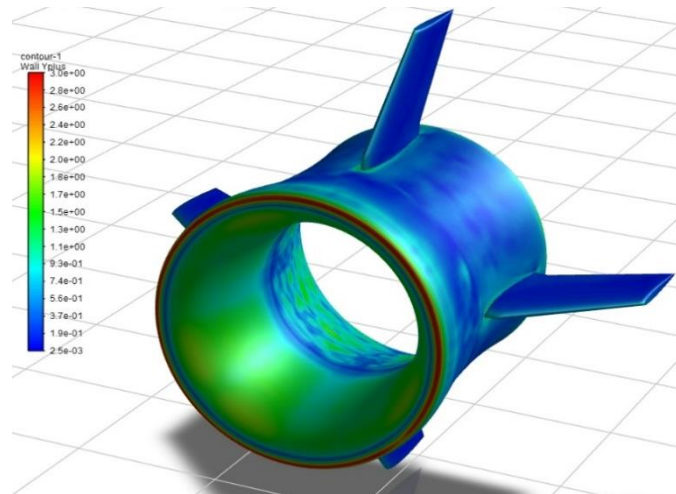
Although the turbine being studied differs in diameter from the smaller turbine used for validation, it is still significant to validate our methodology using a smaller turbine with available experimental data. The purpose of this validation was to demonstrate the accuracy and reliability of the numerical approach, irrespective of the specific turbine size or complexity.

Furthermore, the utilization of LES enables high-resolution analysis of the turbulent flow structures within the turbine wake. By adequately resolving the flow features, our model captures

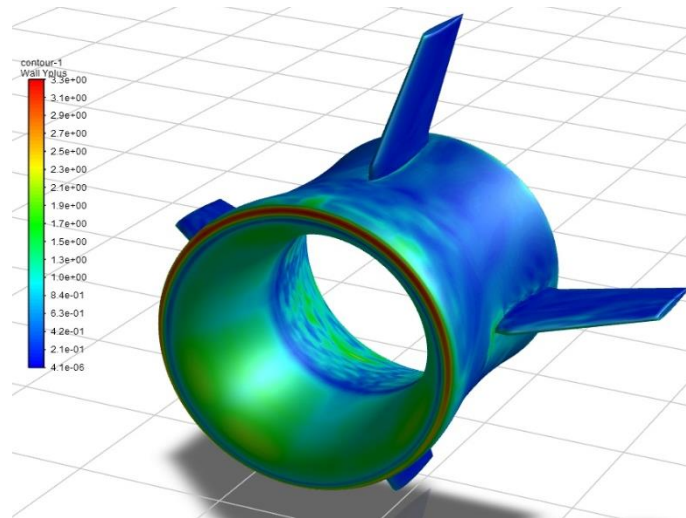
the intricate complexities associated with different turbine sizes. The results obtained from the validation study showcased a satisfactory agreement between the LES-ADM method and experimental measurements. Therefore, in the absence of experimental data for the balloon wind turbine, we argue that validating the robustness of our methodology through promising outcomes obtained using the same approach serves as a reliable indicator of the accuracy of the main model's findings.

6. If the authors claim to use LES, is the energy in the proximity of the balloon wall resolved well?

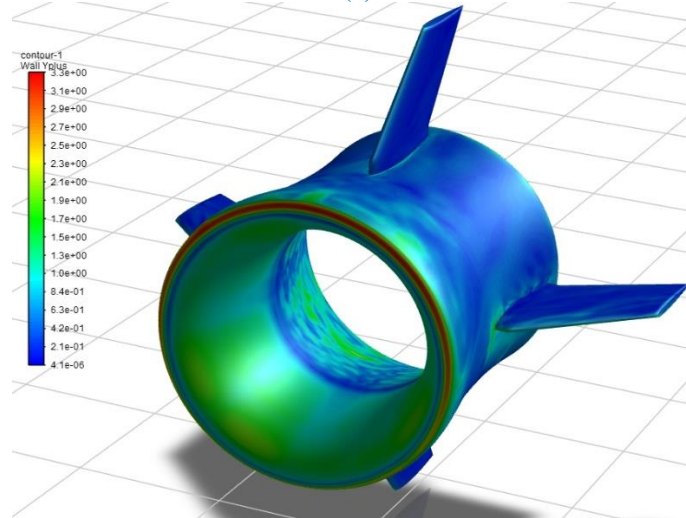
In LES, the y^+ values should be lower than 5 for wall-resolved LES simulations. Moreover, the Dynamic Smagorinsky model tends to perform better in capturing near-wall turbulence compared to traditional static SGS models, as it adapts the SGS model coefficients dynamically based on the local flow characteristics. When using this model, a lower y^+ value (closer to 1) is often recommended for accurate resolution of the near-wall turbulent structures. This is because the model is designed to capture small-scale motions more effectively, and a finer resolution near the wall helps to capture the important energy-containing turbulent eddies. When the y^+ value falls within this range, it generally indicates that the energy near the wall is resolved well. To reach these values near the balloon wall in the simulations, the mesh size and its spacing near the wall were adjusted accordingly. Figure vii illustrates y^+ contours for $U_{ref} = 7 \text{ m s}^{-1}$ and $\theta_{tilt} = 0^\circ, 5^\circ$ and 10° on the balloon wall. According to the figure, the value of this parameter is close to 1 in most regions on the wall and does not exceed 3.5 in any region for different wind scenarios.



(a)



(b)



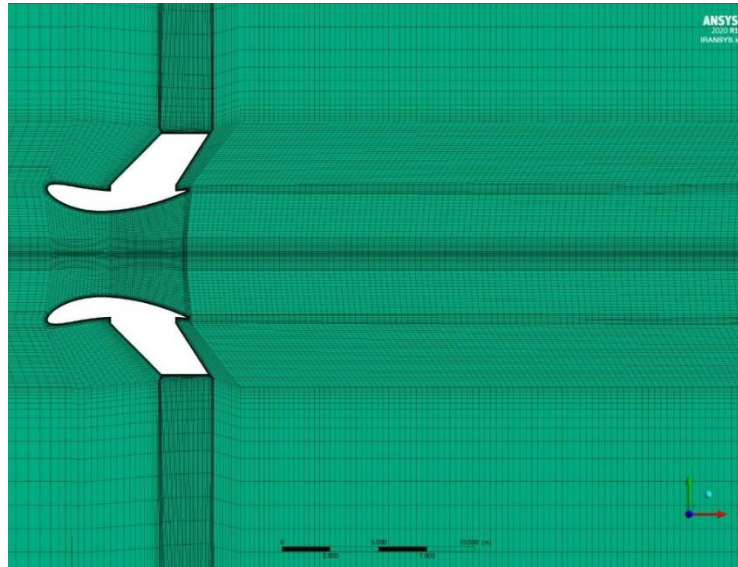
(c)

Figure vii. Wall Yplus contours for $U_{ref} = 7 \text{ m s}^{-1}$ and (a) $\theta_{tilt} = 0^\circ$, (b) $\theta_{tilt} = 5^\circ$ (c) $\theta_{tilt} = 10^\circ$ on the balloon's wall.

- The authors focus the studies on the wake, but the mesh behind the balloon does not seem to be well refined such that it can well resolve small eddies. Perhaps plot the Q or Lambda2 criterion?

To determine the mesh distribution in the wake region, the LES-friendly mesh generation algorithm, which was described in section 5.1 of the manuscript, was adopted. Evidence confirming the reliability and suitability of the mesh generation approach has been provided in response to the third query posed by Referee #2. To further investigate the mesh size in the region of interest, the mesh distribution in the near-wake is illustrated in figure viii (a). To resolve small eddies in the wake of the turbine and the vicinity of the balloon's separation region (close to the trailing edge of the balloon's airfoil), the mesh resolution in these areas

was significantly enhanced compared to other regions within the computational domain, as illustrated in figure viii (a). The magnitude of Λ_2 for the case where $U_{ref} = 7 \text{ m s}^{-1}$ and $\theta_{tilt} = 0^\circ$ in the symmetry plane of the balloon ($z=0$) is clipped for small eddies and the corresponding contour is depicted in figure viii (b). According to figure viii (b), the small eddies in the separation zone of the balloon and the wake of the turbine are properly resolved.



(a)



(b)

Figure viii. (a) Mesh distribution (b) Λ_2 contour on the symmetry plane of the balloon

8. Last minor aspect: remove the 6th point in Conclusion as nothing is written there.

Thank you for pointing out this error; we have removed it.